

Supplementary Information for

Mucinase-engineered cell membrane nanovesicles degrade the glycocalyx shield to potentiate antitumor immunity

Xiaorui Geng^{a,1}, Silan Liu^{a,b,1}, Yuanwei Pan^a, Yun Ge^{a,c,2}, and Lang Rao^{a,2}

^a Institute of Chemical Biology, Shenzhen Bay Laboratory, Shenzhen 518132, China.

^b Shenzhen Medical Academy of Research and Translation (SMART), Shenzhen 518107, China.

^c State Key Laboratory of Chemical Oncogenomics, School of Chemical Biology and Biotechnology, Peking University Shenzhen Graduate School, Shenzhen 518055, China.

¹ X.G. and S.L. contributed equally to this work.

² Corresponding e-mail: geyun@szbl.ac.cn (Y.G.); lrhao@szbl.ac.cn (L.R.).

This PDF file includes:

Supplementary Methods

Tables S1 to S3

Figures S1 to S24

Supplementary Methods

Plasmid and subcloning

All StcE variants, each engineered with a secretion signal sequence, were generated using the pET30a plasmid as a template. SpyCatcher (SC) or StcE variants bearing an N-terminal HA tag were cloned into the pDisplay™ expression vector for cell surface display. Subsequently, constructs containing a signal peptide and the PDGFR β transmembrane domain were subcloned into a lentiviral vector that co-expresses Green Fluorescent Protein (GFP) as a selection marker to facilitate the generation of stable cell lines.

Cell culture and transfection

HEK293T, CT26, 4T1, and RAW264.7 cells were maintained in Dulbecco's Modified Eagle Medium (DMEM) supplemented with 10% fetal bovine serum (FBS) and 1% penicillin–streptomycin. All cell lines were cultured in a humidified incubator at 37 °C with 5% CO₂. Transfections were performed using polyethylenimine (PEI) according to the manufacturer's protocol.

Generation of stable cell lines

Replication-deficient lentivirus was produced by transfecting HEK293T cells at 90% confluency in 6-well plates with a plasmid mixture containing 0.75 μ g of psPAX2, 0.25 μ g of pMD2.G, and 1 μ g of the plasmid encoding the gene of interest. The viral supernatant was collected 48 hours post-transfection and filtered through a 0.45 μ m membrane. For transduction, the filtrate was combined with an equal volume of fresh medium containing 10 μ g/mL polybrene and used to infect the target cells. Forty-eight hours after transduction, cells were harvested, and the GFP-positive population was isolated by fluorescence-activated cell sorting (FACS) using a CytoFLEX SRT instrument (Beckman Coulter).

Protein expression and purification

Protein expression and purification were performed as previously described (1). Briefly, sequence-verified plasmids were transformed into Escherichia coli BL21 (DE3) cells, which were then cultured in sterile medium containing 30 μ g/mL kanamycin. At an OD₆₀₀ of 0.6, protein expression was induced with 0.3 mM IPTG, followed by overnight incubation. Cells were harvested by centrifugation (5,000 \times g, 30 min, 4 °C). The resulting cell pellet was lysed by sonication, and the lysate was clarified by centrifugation (10,000 \times g, 30 min, 4 °C). The supernatant, containing the crude protein, was loaded onto an AKTA purification system. Impurities were removed using a wash buffer (20 mM Tris-HCl pH 7.4, 150 mM NaCl, 40 mM imidazole), and the target protein was eluted with an elution buffer (20 mM Tris-HCl pH 7.4, 150 mM NaCl, 250 mM imidazole). The purified protein was dissolved into PBS and stored at -80 °C.

Silver staining of StcE-treated C1INH

As previously reported (2), C1INH (Novoprotein) was treated with StcE variants at a 1:10 enzyme-to-substrate (E/S) mass ratio in 50 mM ammonium bicarbonate. The reaction was incubated at 37 °C for 3 hours in a total volume of 15 µL. Reaction products (0.5 µg) were separated by SDS-PAGE (150 V, 1 hour) and visualized using a Fast Silver Stain Kit (Beyotime) according to the manufacturer's protocol.

Preparation of cell membrane nanovesicles

Cell membrane nanovesicles (NVs) were prepared from HEK293T-SC, HEK293T-StcE, 4T1, 4T1-nCD47, CT26, and CT26-nCD47 cells. Cells were harvested and subjected to three rapid freeze-thaw cycles using liquid nitrogen for freezing and a room-temperature water bath for thawing. The resulting lysate was clarified by centrifugation at 4,000 × g for 45 min at 4 °C. The supernatant was then ultracentrifuged at 100,000 × g for 1 h at 4 °C to pellet crude vesicles. To achieve a uniform size distribution, the crude vesicle pellet was resuspended in PBS. The suspension was sonicated on ice for 5 minutes (50 W; 2 s on, 4 s off pulse cycle), followed by sequential extrusion (10 passes each) through 200 nm and then 100 nm polycarbonate membranes using a mini-extruder. The final single-source NV products were designated as NVs (derived from HEK293T, 4T1 and CT26), StcE-NVs (derived from HEK293T-StcE) and nCD47-NVs (derived from 4T1/CT26-nCD47). Fused nanovesicles (FNVs) were generated by combining different NV preparations at the mass ratios specified in *Table 2*. This mixture was then subjected to the same sonication and extrusion procedure described above to induce membrane fusion and ensure homogeneity. The resulting FNV products included FNVs, StcE-FNVs, nCD47-FNVs and StcE-nCD47-FNVs. The protein concentration of all vesicle preparations was quantified using a BCA protein assay kit (Thermo Fisher).

Characterization of NVs

For morphological analysis by transmission electron microscopy (TEM), 10 µL of a vesicle suspension was applied to a copper grid, air-dried, and negatively stained with 2% phosphotungstic acid for 3 minutes. The hydrodynamic diameter and zeta potential of the vesicles were measured by dynamic light scattering (DLS) using a Malvern Zetasizer instrument.

Western blot analysis of bio-ligation on the surface of cells and NVs

To analyze surface conjugation, cells and cellular nanovesicles (NVs) were lysed in RIPA buffer. Total protein concentration was quantified using a bicinchoninic acid (BCA) assay kit (Thermo Fisher). Equal amounts of denatured protein lysate were separated on a 10% SDS-polyacrylamide gel and subsequently transferred to a nitrocellulose membrane using an eBlot™ L1 system (Genscript). The membrane was blocked with 5% (w/v) non-fat dry milk in TBST for 1 hour at room temperature. Membranes were then incubated with primary antibodies overnight at

4 °C, followed by incubation with an HRP-conjugated secondary antibody for 1 hour at room temperature. Blots were visualized using an Azure Imager C600, and band densitometry was performed using Fiji software.

Conjugation of SpyCatcher with SpyTag

For *in vitro* conjugation, recombinant SpyCatcher (SC) and SpyTag (ST)-labeled StcE variants were incubated in PBS (pH 7.4) containing 1% (w/v) BSA on ice for 25 minutes with periodic mixing. Reactions were quenched by adding 5× SDS-PAGE loading buffer and heating at 95 °C for 5 minutes. Conjugation efficiency was assessed by 8% SDS-PAGE. For cell-surface conjugation, HEK293T-SC cells were detached using 0.25% trypsin and incubated with ST-labeled StcE variants in PBS containing 1% BSA for 25 minutes on ice. To remove unbound protein, cells were washed twice with PBS. The extent of conjugation was determined by staining the cells with a His-tag primary antibody followed by a fluorophore-conjugated secondary antibody and analyzing them by flow cytometry (data processed with FlowJo software).

Flow cytometry analysis of demucinated cancer cells

Tumor cells were treated with either purified StcE variants or with HEK293T-SC cells/vesicles that had been pre-conjugated with ST-labeled proteins. For the assay, one million tumor cells per sample were incubated in 1 mL of complete medium or PBS containing specified concentrations of purified protein or NVs for 1 hour at 37 °C. In co-culture experiments, HEK293T cells expressing StcE were added at a 2:1 ratio relative to tumor cells. Following treatment, cells were washed with ice-cold FACS buffer and stained with fluorophore-conjugated antibodies for 30 minutes at 4 °C. For co-cultures with EGFP-expressing HEK293T-StcE cells, the EGFP-negative tumor cell population was gated for analysis of cell-surface mucin intensity. Data were acquired on a flow cytometer and analyzed using FlowJo software.

Cell immunofluorescence

CT26, CT26 CD47-knockdown (CD47-KD), 4T1, and 4T1 CD47-knockdown (4T1-KD) cells were seeded into 8-well confocal dishes at a density of 5×10^4 cells/well. After 12 hours, each well was treated with 120 µg of the corresponding vesicle formulation (NVs, nCD47-NVs and StcE-nCD47-FNVs) in 300 µL of medium for 1 hour. Following treatment, the cells were washed twice with PBS and fixed with 4% paraformaldehyde for 15 minutes. The cell membranes were then stained with WGA-Alexa Fluor 647 (WGA-AF647) for 15 minutes at room temperature. After washing, cells were blocked with 5% BSA in PBS for 1 hour at room temperature and then incubated with an anti-HA primary antibody overnight at 4°C. The next day, cells were washed twice with PBS and incubated with a FITC-conjugated secondary antibody for 1 hour at room temperature. Finally, nuclei were counterstained with DAPI for 15 minutes. After a final wash, serum-free medium was

added to each well, and images were acquired using a Zeiss LSM 980 confocal microscope equipped with a 40x objective.

Phagocytosis assay

RAW264.7 macrophages were stimulated with lipopolysaccharide (LPS, 200 ng/mL) for 24 hours, labeled with CFSE (eBioscience™), and seeded into 4-chamber confocal dishes. In parallel, 4T1 or CT26 cancer cells were harvested, stained with eFluor™ 670 proliferation dye, and treated with the indicated nanovesicle (NV) formulations for 3 hours at 37°C. These vesicle-treated cancer cells were then washed and co-cultured with the prepared RAW264.7 macrophages for 6 hours. After co-incubation, the cells were washed with PBS, fixed with 4% paraformaldehyde, and imaged on a Zeiss LSM980 confocal microscope. Images were subsequently processed and analyzed using Fiji software.

Animal model for *in vivo* experiments

Female BALB/c mice (6–8 weeks) were purchased from GemPharmatech Co., Ltd. and housed in a specific pathogen-free (SPF) facility. All animal procedures were conducted in accordance with guidelines approved by the Regional Ethics Committee for Animal Experiments at Shenzhen Bay Laboratory (Permit No. AERL202203). For the subcutaneous tumor model, mice were injected in the right flank with 5×10^5 CT26 cells. *In vivo* biodistribution studies were performed 10 days post-inoculation. Therapeutic efficacy studies were initiated 7 days post-inoculation. For the lung metastasis model, mice were injected via the tail vein with 2×10^5 4T1-luciferase expressing (4T1-luc) cells. Metastatic progression was monitored by measuring bioluminescence signals from the thoracic region on days 0, 9, 15, and 21 using an IVIS *in vivo* imaging system (Xenogen Corp).

Biocompatibility of StcE-nCD47-FNVs

The biocompatibility of StcE and StcE-nCD47-FNVs (derived from HEK293T-StcE and CT26-nCD47 cells) was evaluated using hemolysis and cytotoxicity assays, followed by *in vivo* toxicity assessment. For the hemolysis assay, red blood cells (RBCs) were collected from the whole blood of healthy BALB/c mice and suspended in PBS. The RBC suspension was incubated with various concentrations of StcE or StcE-nCD47-FNVs (10-1000 µg/mL) at 37 °C for 2 h. PBS and deionized water served as negative and positive controls, respectively. After incubation, the samples were centrifuged at 10,000 rpm for 2 min, and the absorbance of the supernatant was measured at 540 nm to determine hemoglobin release. The percentage of hemolysis was calculated using a standard equation. The cytotoxicity of StcE and StcE-nCD47-FNVs was assessed using the bEnd.3 murine brain endothelioma cell line. Cells were seeded into 96-well plates at a density of 8,000 cells per well. After 12 hours, the culture medium was replaced with serum-free medium containing various concentrations of the test agents (0–50 µg/mL). Following

a 6-hour incubation, cell viability was quantified using a Cell Counting Kit-8 (CCK-8) assay according to the manufacturer's protocol. To evaluate potential systemic toxicity, CT26 tumor-bearing mice ($n=6$ per group) received intravenous injections of StcE or StcE-nCD47-FNVs via the tail vein. At the study endpoint, blood was collected for a complete blood count (CBC) and serum biochemical analysis to assess hematological parameters and organ function. Key organs, including the heart, liver, spleen, lungs, and kidneys, were harvested, fixed in 10% neutral buffered formalin, and processed for histopathological examination using hematoxylin and eosin (H&E) staining to evaluate tissue morphology.

***In Vivo* biodistribution**

For fluorescent labeling of proteins and NVs: the StcE protein was fluorescently labeled with NHS-Cy5.5 at a 1:10 protein-to-dye molar ratio by incubating the mixture for 2 hours at 37°C. Unconjugated dye was subsequently removed using a desalting column. The labeled protein was then concentrated to 1 mg/mL using an ultrafiltration device with a 10 kDa molecular weight cutoff (MWCO). Various nanovesicle formulations (StcE-NVs, CT26-nCD47-NVs, and CT26-StcE-nCD47-FNVs) were labeled by incubating 1 mg of vesicles with 100 µg of the lipophilic dye DSPE-PEG-Cy5.5 in 1 mL of PBS. The mixture was incubated for 20 minutes at 37°C with continuous shaking, followed by 10 minutes of bath sonication to facilitate dye insertion into the vesicle membranes(3). Biodistribution studies were conducted in CT26 tumor-bearing BALB/c mice 10 days after tumor cell inoculation. Mice were randomly assigned to four groups ($n=3$ per group) to receive intravenous injections of Cy5.5-labeled StcE, StcE-NVs, CT26-nCD47-NVs, or CT26-StcE-nCD47-FNVs. Whole-body fluorescence images were acquired at 0.5-, 1-, 2-, 4-, 6-, 12-, 24-, 36-, and 48-hours post-injection using an IVIS imaging system. At the 48-hour endpoint, mice were euthanized, and the tumors and major organs were harvested for *ex vivo* fluorescence signal quantification.

***In Vivo* therapeutic efficacy in the CT26 subcutaneous tumor model**

Seven days after tumor inoculation, fifty-six CT26 tumor-bearing mice were randomized into five treatment groups to receive intravenous injections of: PBS (vehicle control, $n=13$), CT26-FNVs ($n=10$), CT26-StcE-FNVs ($n=10$), CT26-nCD47-NVs ($n=10$), or CT26-StcE-nCD47-FNVs ($n=13$). Each dose consisted of a 120 µL injection volume containing 120 µg of the respective agent. Treatments were administered every other day for a total of six doses. Body weight and tumor volume were monitored every other day starting on day 5. Mice were euthanized when tumor volume exceeded 1500 mm³, which was defined as the endpoint for survival analysis. A subset of mice from each group was monitored for a long-term survival study.

Flow cytometry analysis of intratumoral immune Cells

On day 19 post-inoculation, tumors ($n=4$ per group) were excised and dissociated into single-cell suspensions for immune profiling. Tissues were mechanically minced and then enzymatically digested for 40 minutes in a buffer containing DNase I (25 U/mL), Collagenase (0.2 mg/mL), and Hyaluronidase (0.1 mg/mL). The digest was further processed using a gentleMACS Dissociator. The resulting cell suspension was filtered through a 70 μ m cell strainer, and contaminating red blood cells were removed by incubation with RBC Lysis Buffer (Solarbio). After quantification, 2×10^6 cells per sample were stained with antibody panels to identify T cell, macrophage, and NK cell populations, as detailed in the Supplementary Table 1 and Figure S17-S18. Intracellular staining for Foxp3 and Granzyme B (GranB) was performed using a commercial fixation and permeabilization kit according to the manufacturer's protocol.

Analysis of inflammatory cytokine levels

For ELISA assay, tumor tissues of equivalent weight were excised from each treatment group of the CT26 tumor-bearing mice, snap-frozen in liquid nitrogen, and stored at -80°C . For analysis, frozen tissues were homogenized in ice-cold PBS containing a protease inhibitor cocktail. The homogenates were further lysed by sonication (5 min, 4°C) and then clarified by centrifugation ($10,000 \times g$, 15 min, 4°C). The concentrations of IFN- γ , Interleukin-6 (IL-6), Interleukin-10 (IL-10), and TGF- β in the resulting supernatants were quantified using commercial ELISA kits according to the manufacturer's protocols. For quantitative Real-Time PCR (qRT-PCR) assay, mRNA levels of inflammatory cytokines in 4T1 lung tissues were measured. Total RNA was extracted from cryopreserved tissues using a commercial RNA extraction kit, and cDNA was subsequently synthesized using the iScript™ cDNA Synthesis Kit (Bio-Rad). qRT-PCR was performed using SYBR Green SuperPremix on a CFX96 Real-Time System (Bio-Rad). Gene expression was normalized to the housekeeping gene GAPDH, and relative expression levels were calculated using the $2^{-\Delta\Delta\text{CT}}$ method. All primers (Supplementary Table 2) were synthesized by BGI Co., Ltd.

RNA sequence

On day 12, tumor tissues were harvested from three randomly selected mice from the vehicle control and CT26-StcE-nCD47-FNVs treatment groups. The tissues were immediately snap-frozen and stored at -80°C . Total RNA extraction, library preparation, sequencing, and bioinformatics analysis were performed by Novogene Co., Ltd. (Beijing, China).

Immunofluorescence

Lung tissues were collected from the 4T1 lung metastasis mouse model, fixed overnight in 4% paraformaldehyde at 4°C , and embedded in paraffin. Paraffin-embedded sections were deparaffinized, rehydrated, and subjected to antigen retrieval. Sections were then blocked with serum for 1 hour at room temperature and incubated overnight at 4°C with primary antibodies against CD4, CD8, CD206, or CD86. After washing, sections were incubated with corresponding

fluorophore-conjugated secondary antibodies for 1 hour. Nuclei were counterstained with DAPI, and images were acquired on an Olympus VS200 fluorescence microscope.

Statistical analyses

Data are presented as mean \pm standard deviation (SD) unless otherwise specified. Statistical analyses were performed using GraphPad Prism (v. 10.1.2). Comparisons between multiple groups were conducted using a one-way analysis of variance (ANOVA) followed by Tukey's post hoc test. For experiments with two independent variables, a two-way ANOVA with Tukey's post hoc test was used. Survival curves were generated using the Kaplan-Meier method and compared using the log-rank (Mantel-Cox) test. A *p-value* < 0.05 was considered statistically significant. Significance levels are denoted as follows: **P* < 0.05, ***P* < 0.01, ****P* < 0.001, and *****P* < 0.0001.

Data availability

The data that support the findings of this study are available from the corresponding author upon reasonable request.

Reference

1. K. Pedram *et al.*, Design of a mucin-selective protease for targeted degradation of cancer-associated mucins. *Nat. Biotechnol.* **42**, 597-607 (2024).
2. S. A. Malaker *et al.*, The mucin-selective protease StcE enables molecular and functional analysis of human cancer-associated mucins. *Proc. Natl. Acad. Sci.* **116**, 7278–7287 (2019).
3. J. C. Wu, H. L. Lu, X. M. Xu, L. Rao, Y. Ge, Engineered cellular vesicles displaying glycosylated nanobodies for cancer immunotherapy. *Angew. Chem. Int. Ed. Engl.* **63**, e202404889 (2024).

Supplementary Tables

Table S1. Main reagents and materials

Reagents	Source	Identifier
Live/Dead-BV510	BD Pharmingen	564406
CD45-APC-CY7	BD Pharmingen	557659
CD3-FITC	BD Pharmingen	553061
CD4-BV650	Biolegend	100555
CD8-BV605	BD Pharmingen	563152
GranB-APC	Biolegend	372204
Foxp3-PE	BD Pharmingen	563101
CD11b-FITC	BD Pharmingen	553310
F4/80-APC-R700	BD Pharmingen	565787
CD86-BV650	BD Pharmingen	564200
CD206-AF647	Biolegend	141712
CD49b-PE	BD Pharmingen	558759
MUC1-PE	Biolegend	355604
HA-pacific blue	Biolegend	901526
eBioscience™ cell proliferation Dye eFlour™ 670	Invitrogen	65-0840-85
His-APC	Biolegend	362605
CD47-PE	Biolegend	127508
anti-HA Rb	CST	3724
anti-His Ms	Proteintech	66005
anti-GAPDH Rb	HUABIO	ET1601-4
CFSE	Invitrogen	C34554

Table S2. List of main abbreviations

Abbreviation	Description
StcE	Secreted protease of C1 esterase inhibitor
C1INH	C1 esterase inhibitor
AF647	Alexa Fluor 647
SC	SpyCatcher003
ST	SpyTag003
NVs	Derived from HEK293T /CT26/4T1 cells, no functional proteins
StcE- NVs	Derived from HEK293T-StcE cells, glycocalyx hydrolysis only
nCD47-NVs	Derived from CT26/4T1-nCD47 cells, CD47 blockade only
FNVs	HEK293T-NVs and NVs were fused at 1:3 mass ratio, no functional proteins
StcE-FNVs	StcE-NVs and NVs were fused at 1:3 mass ratio, glycocalyx hydrolysis only
nCD47-FNVs	HEK293T-NVs and nCD47-NVs were fused at 1:3 mass ratio, CD47 blockade only
StcE-nCD47-FNVs	StcE-NVs and nCD47-NVs were fused at 1:3 mass ratio, combination of glycocalyx hydrolysis and CD47 blockade

Table.S3. Primers for qRT-PCR

Primer	Sequence
IFN- γ . <i>F</i>	CAGCAACAGCAAGGCGAAAAAGG
IFN- γ . <i>R</i>	TTTCCGCTTCCTGAGGCTGGAT
TNF- α . <i>F</i>	GGTGCCTATGTCTCAGCCTCTT
TNF- α . <i>R</i>	GCCATAGAACTGATGAGAGGGAG
IL-1 β . <i>F</i>	TGGACCTTCCAGGATGAGGACA
IL-1 β . <i>R</i>	GTTTCATCTCGGAGCCTGTAGTG
IL-10. <i>F</i>	CGGGAAGACAATAACTGCACCC
IL-10. <i>R</i>	CGGTTAGCAGTATGTTGTCCAGC
GAPDH. <i>F</i>	CATCACTGCCACCCAGAAGACTG
GAPDH. <i>R</i>	ATGCCAGTGAGCTTCCCGTTCAG
CD47. <i>F</i>	GGTGGGAACTACACTTGCGAAG
CD47. <i>R</i>	CTCCTCGTAAGAACAGGCTGATC

Supplementary Figures

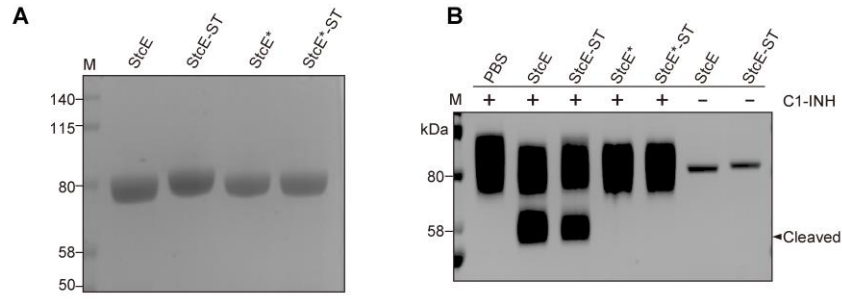


Fig. S1. Expression and enzymatic activity of StcE and StcE variants. (A) Coomassie blue staining of StcE, SpyTag-labeled StcE (StcE-ST), and ST-labeled inactive point mutant StcE* (StcE*-ST) (~80 kDa). (B) Mucinase activity assessed using C1-INH as substrate. Samples treated with StcE, StcE*, StcE-ST, or StcE*-ST (enzyme-to-substrate ratio 1:10) were visualized by silver staining. Cleaved products are indicated. StcE*: inactive mutant.

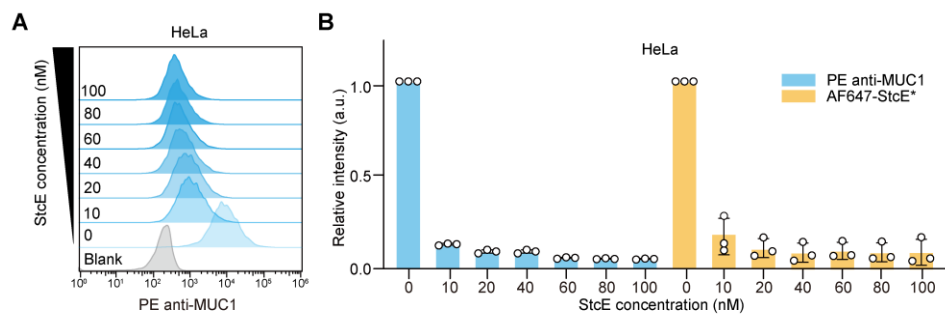


Fig. S2. StcE-mediated degradation of cell-surface mucins on HeLa cells. (A) Flow cytometry analysis of mucin levels after treatment with different StcE concentrations. (B) Normalized mucin intensity quantification using two staining reagents, $n = 3$. Data are mean \pm S.D. StcE*: StcE inactive mutant.

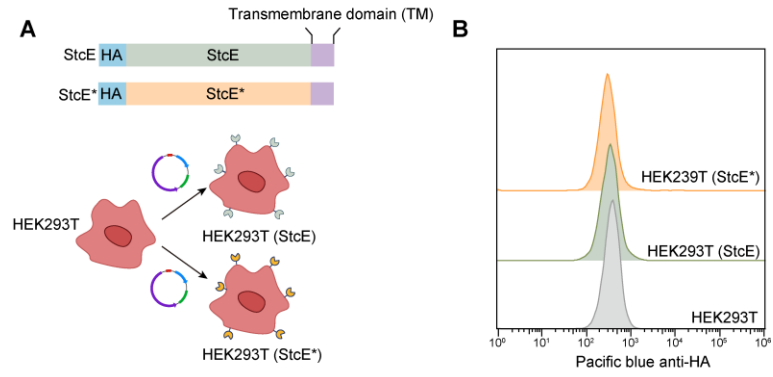


Fig. S3. Genetic display of StcE/StcE* on HEK293T cell surfaces. (A) Schematic of StcE display using pDisplay™-derived constructs with a transmembrane (TM) domain. (B) Flow cytometry of HA-tagged StcE/StcE* in engineered HEK293T stable transfected cells. StcE*: StcE inactive mutant.

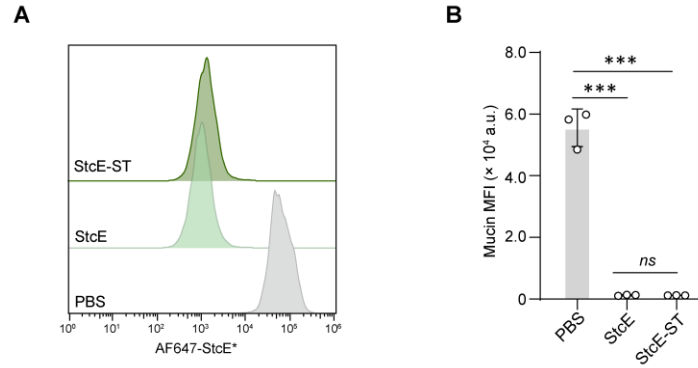


Fig. S4. Comparison of mucinase activity between StcE and ST-labeled StcE. (A) Flow cytometry analysis of HeLa cells-surface mucins after treatment. (B) Mean fluorescence intensity (MFI) quantification, $n = 3$. Statistical significance: unpaired two-tailed Student's t-test. Data are mean \pm S.D. StcE*: StcE inactive mutant. *ns*: not significant; *** $P < 0.001$.

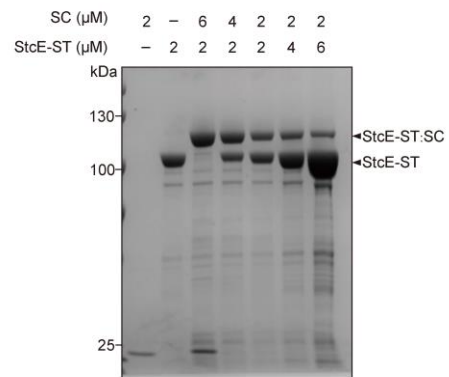


Fig. S5. *In vitro* bioconjugation of StcE-SpyTag (ST) with SpyCatcher (SC). SC was incubated with StcE-ST for 25 min, analyzed by SDS-PAGE with coomassie staining.

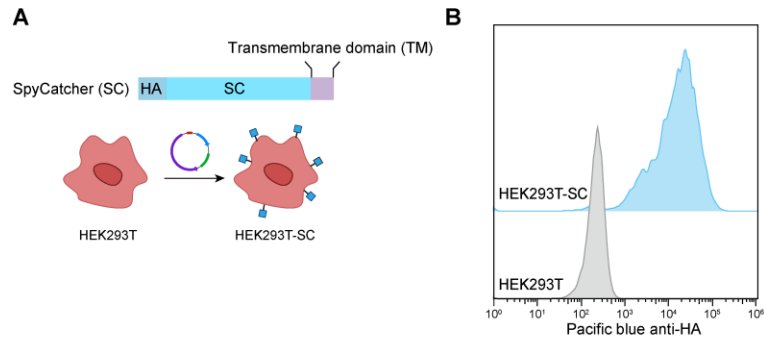


Fig. S6. SpyCatcher (SC) display on HEK293T cells. (A) Schematic of SC display using pDisplay™-derived constructs containing a TM domain. (B) Flow cytometry of HA-tagged SC on engineered HEK293T cells.

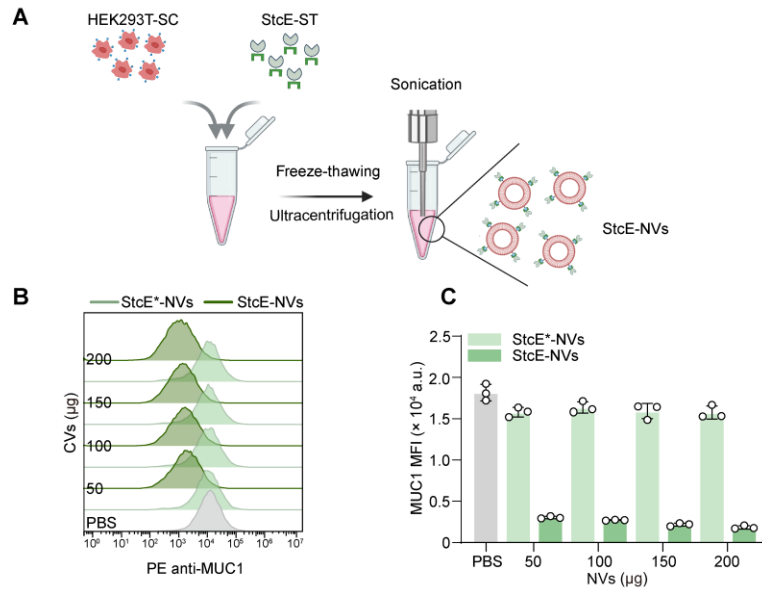


Fig. S7. Preparation and activity validation of StcE-NVs. (A) Schematic illustration of StcE-NVs preparation. (B) Flow cytometry analysis and (C) MFI quantification of MUC1 on HeLa cells after treatment with StcE-NVs, stained with PE-labelled anti-MUC1 antibody. StcE*: StcE inactive mutant.

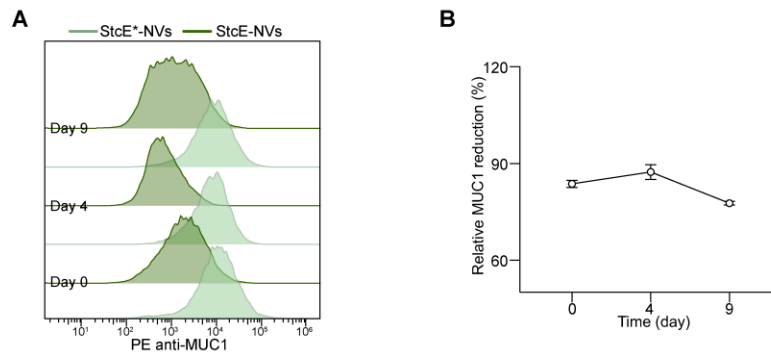


Fig. S8. Stability of StcE-NVs for 7 days. (A) Flow cytometry of MUC1 on HeLa cells after incubation with StcE-NVs or StcE*-NVs at day 0, 4, 9. (B) Change of the MUC1 protein level, $n = 3$. Data mean \pm S.D. StcE*: StcE inactive mutant.

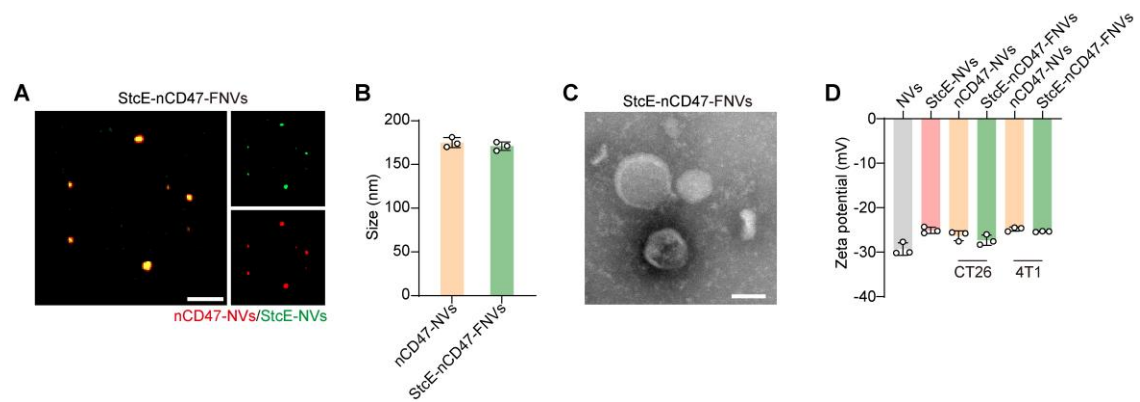


Fig. S9. Fusion of nCD47-NVs with StcE-NVs and characterization of 4T1-StcE-nCD47-FNVs. (A) CLSM images of fusion of Dil-labeled 4T1-nCD47-NVs (red) with DiO-labeled StcE-NVs (green). Scale bar, 5 μ m. (B) Size distribution of 4T1-nCD47-NVs and 4T1-StcE-nCD47-FNVs. (C) TEM image of 4T1-StcE-nCD47-FNVs. Scale bar, 50 nm. (D) Zeta potential of HEK293T-NVs, StcE-NVs, CT26-nCD47-NVs, CT26-StcE-nCD47-FNVs, 4T1-nCD47-NVs, and 4T1-StcE-nCD47-FNVs.

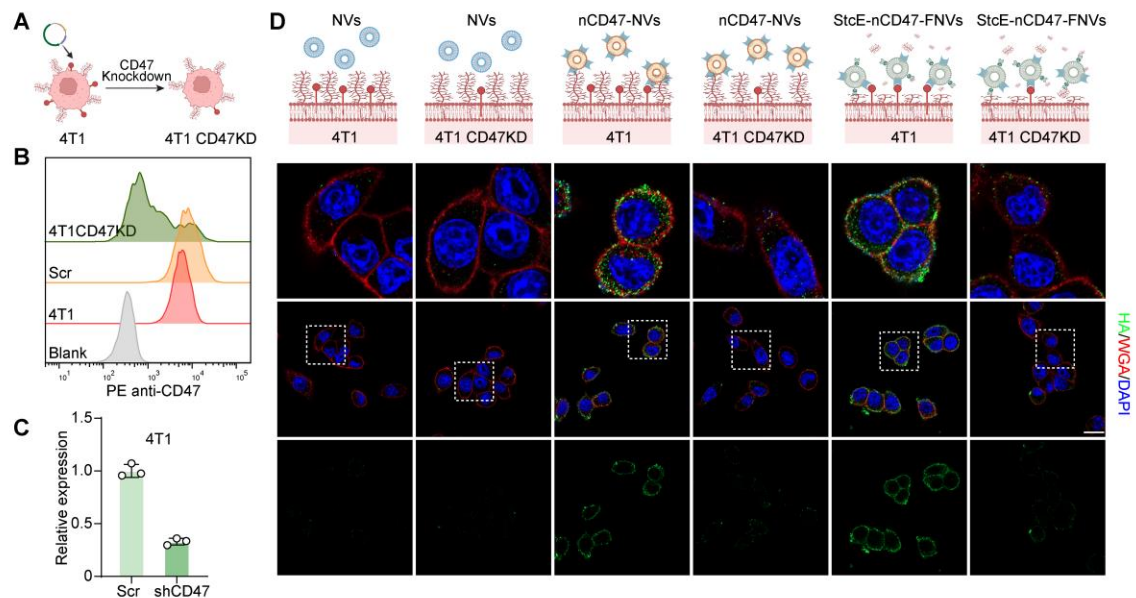


Fig. S10. CD47 knockdown in 4T1 cells and StcE-nCD47-FNVs binding. (A) Schematic of shRNA-mediated CD47 knockdown. (B) Flow cytometry of CD47 in 4T1 cells stably transfected with shScramble (Scr) or shCD47 RNA. (C) qPCR quantification of CD47 mRNA, $n = 3$. (D) Confocal imaging of 4T1-NVs, 4T1-nCD47-NVs or 4T1-StcE-nCD47-FNVs binding to CD47. Scale bar, 20 μ m.

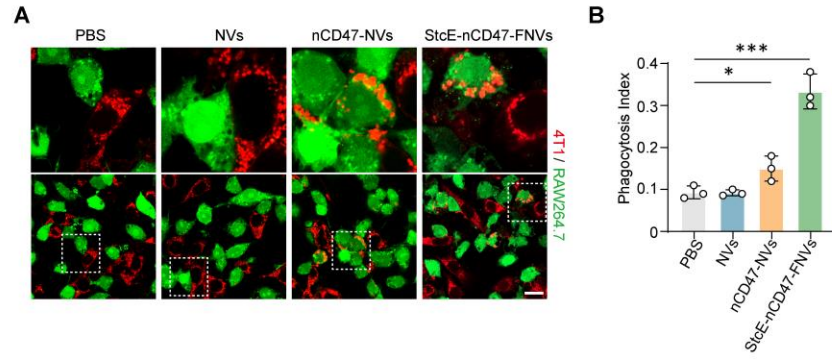


Fig. S11. CD47 blockade enhances macrophage-mediated phagocytosis *in vitro*. (A) Fluorescence images: RAW 264.7 macrophages (CFSE, green) and 4T1 cells (eFluor 670, red). Insets were magnified. Scale bar, 10 μ m. (B) Phagocytosis index (CFSE⁺ 4T1 cells per 50 macrophages), $n = 3$. Data mean \pm S.D.; unpaired two-tailed Student's t-test. * $P < 0.05$, ** $P < 0.01$, *** $P < 0.001$. NVs and nCD47-NVs are from 4T1 and 4T1-nCD47 cells.

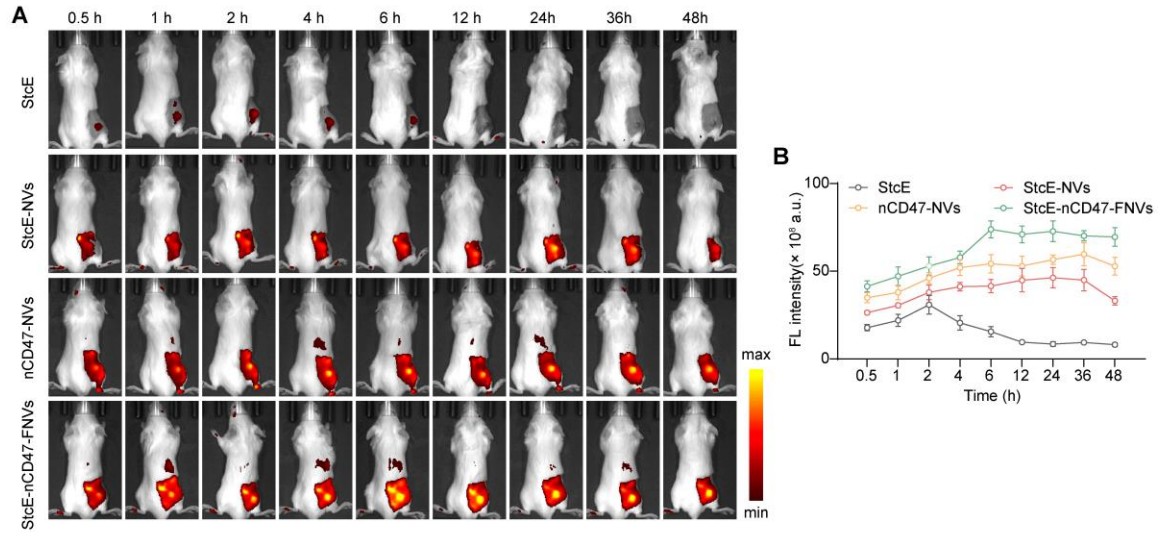


Fig. S12. ***In vivo* biodistribution and tumor accumulation.** (A) Representative *in vivo* fluorescence images (0.5–48 h) after Cy5.5-labeled StcE, StcE-NVs, CT26-nCD47-NVs, CT26-StcE-nCD47-FNVs injection. (B) Tumor fluorescence quantification, $n=3$.

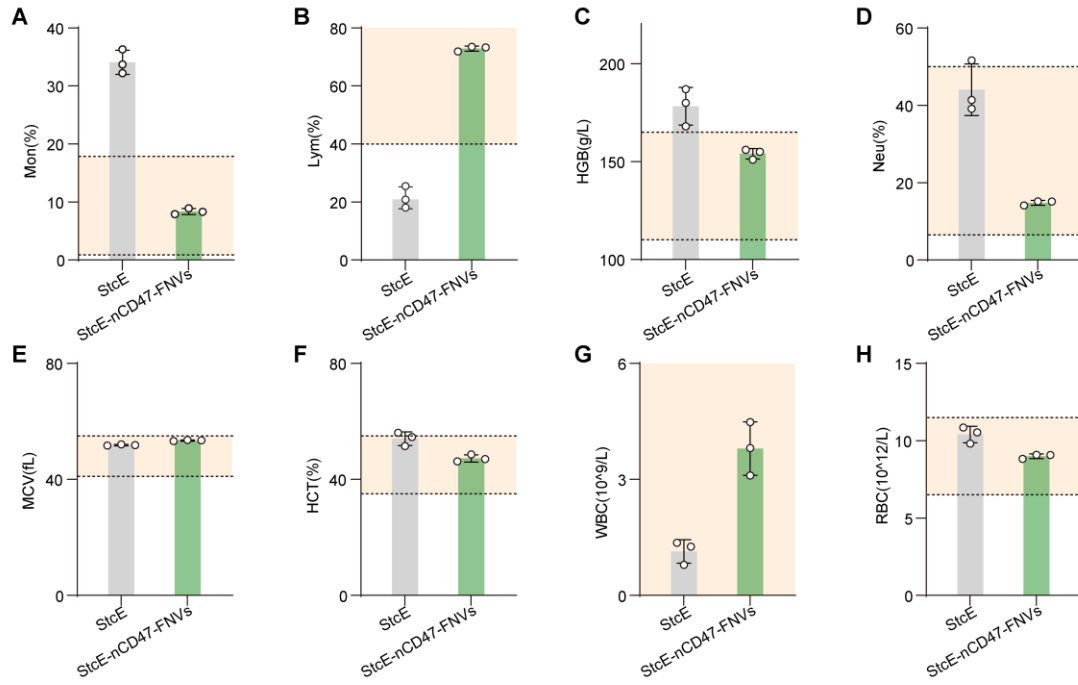


Fig. S13. Hematological analysis of CT26 tumor-bearing mice after intravenous injection of StcE or StcE-nCD47-FNVs. Parameters from a complete blood count (CBC) were measured, including: (A) monocytes (Mon), (B) lymphocytes (Lym), (C) hemoglobin (HGB), (D) neutrophils (Neu), (E) mean corpuscular volume (MCV), (F) hematocrit (HCT), (G) white blood cells (WBC), and (H) red blood cells (RBC). Normal ranges: orange shading, $n = 3$. Data mean \pm S.D. StcE-nCD47-FNVs (HEK293T-StcE-NVs: CT26-nCD47-NVs = 1:3).

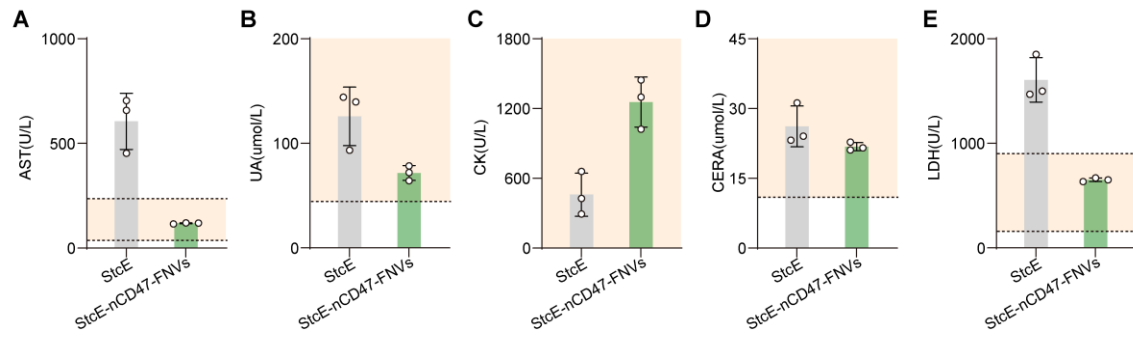


Fig. S14. Blood biochemistry analysis of CT26 tumor-bearing mice after StcE or StcE-nCD47-FNVs treatment. Serum levels of markers for liver function (A: AST), kidney function (B: UA, D: CREA), and general tissue or muscle damage (C: CK, E: LDH) were quantified. Normal ranges: orange shading. Data mean \pm S.D, $n = 3$. StcE-nCD47-FNVs (HEK293T-StcE-NVs: CT26-nCD47-NVs = 1:3).

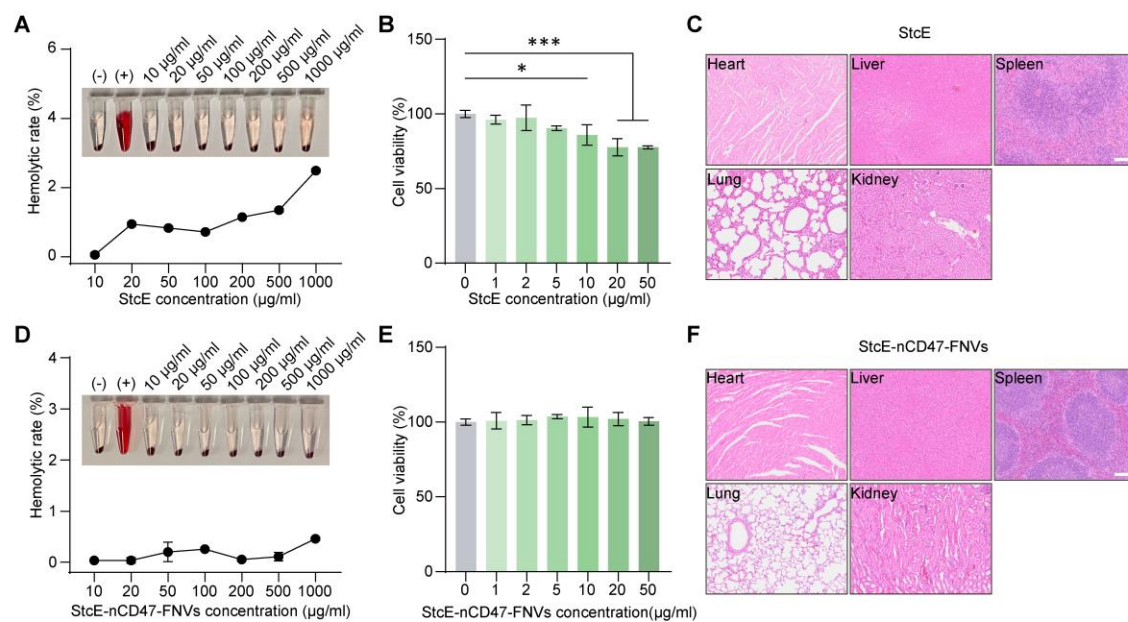


Fig. S15. Biocompatibility of StcE and StcE-nCD47-FNVs. (A, D) Red blood cell hemolysis. (B, E) bEnd.3 cell viability after 6 h incubation. (C, F) H&E-staining sections of major organs. Scale bars, 100 µm. StcE-nCD47-FNVs (HEK293T-StcE-NVs: CT26-nCD47-NVs =1:3).

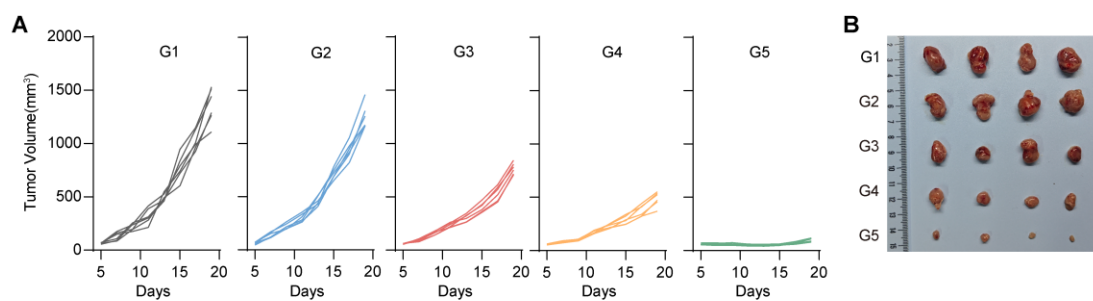


Fig. S16. *In vivo* anti-tumor efficacy of CT26 tumor-bearing mice. (A) Tumor growth curves of CT26 tumor-bearing mice received different treatments. (B) Representative images of tumors from all groups at the experimental endpoint. Related to Fig. 4.

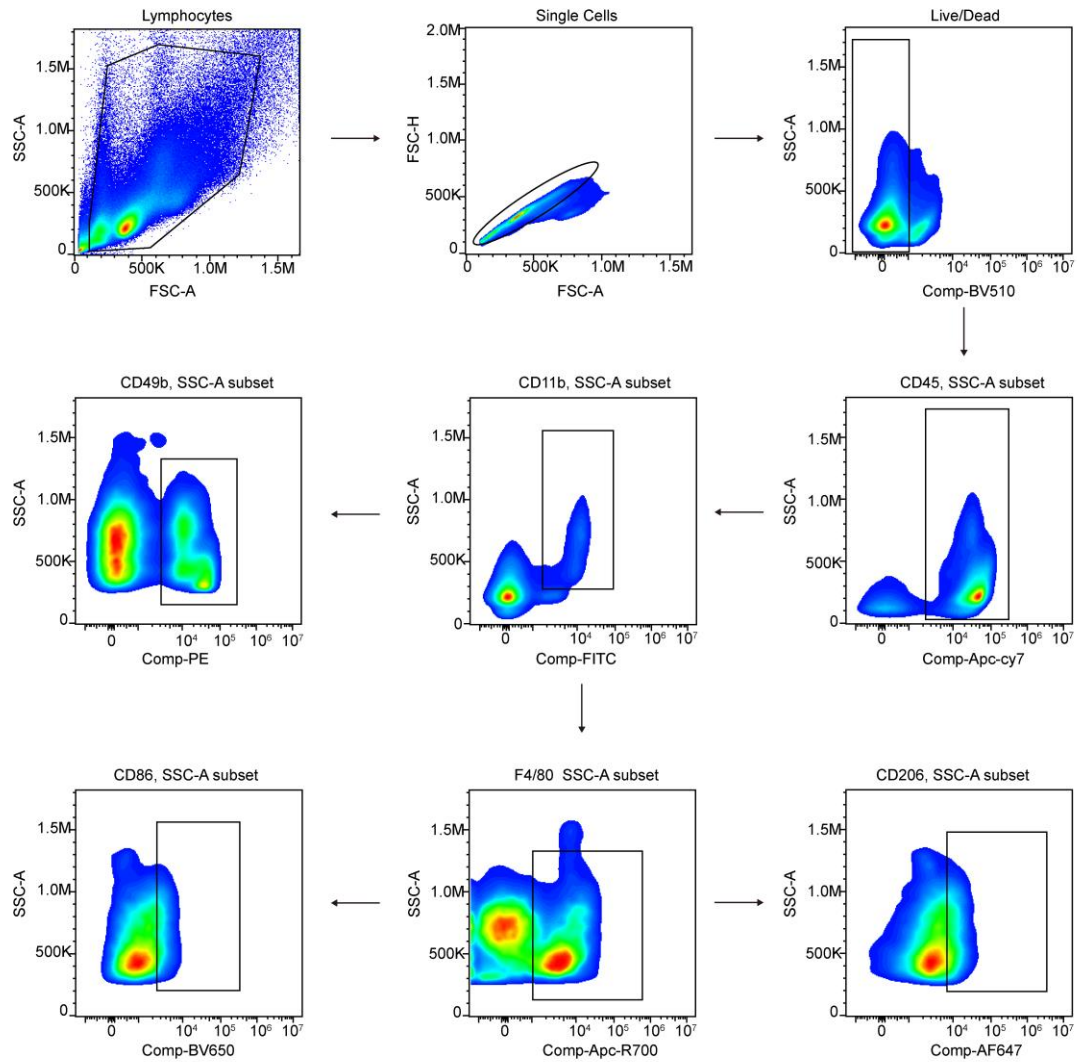


Fig. S17. Gating strategy for flow cytometry of macrophages and NK cells. Related to Fig. 4, S19, S21.

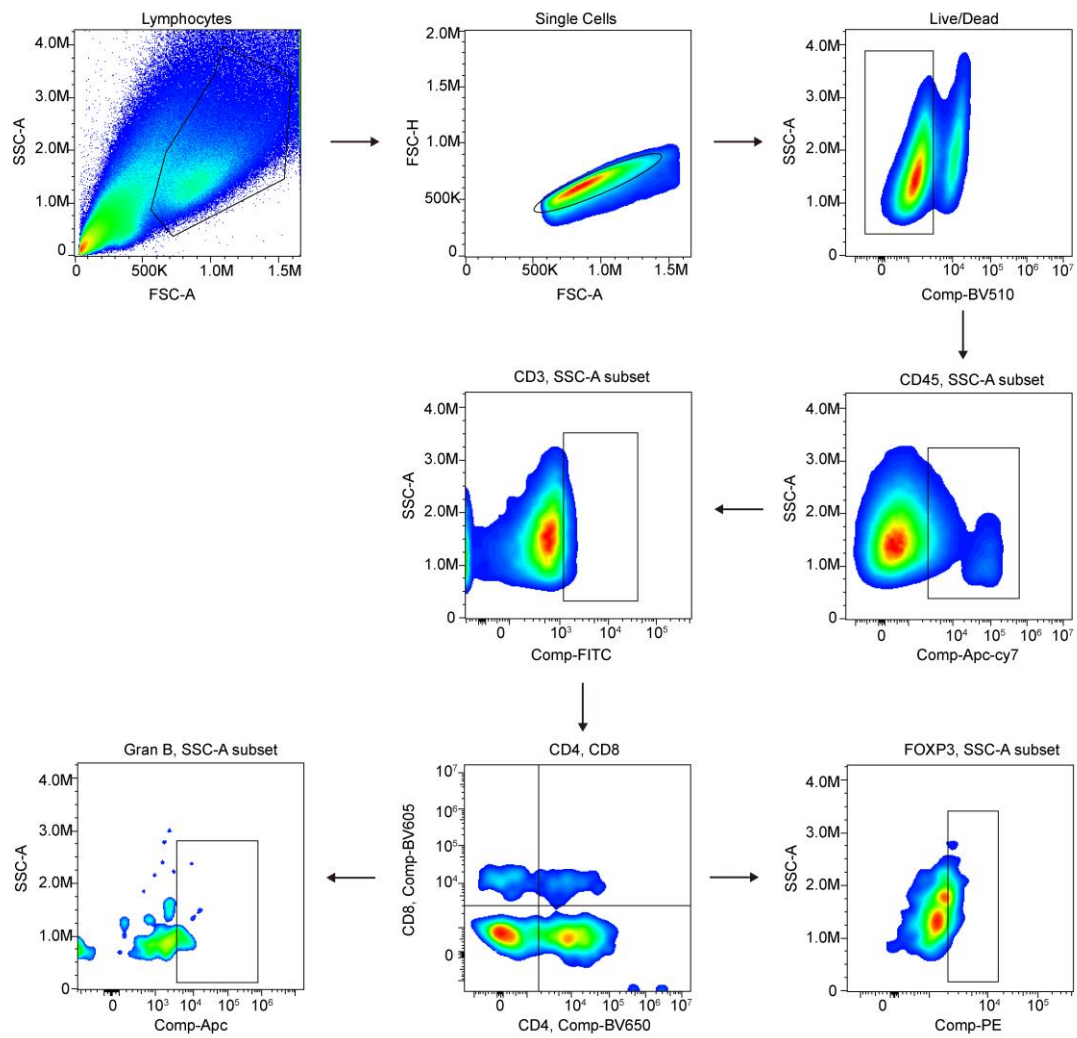


Fig. S18. Gating strategy for flow cytometry of tumor-infiltrating T cells. Related to Fig.4, S20, S21.

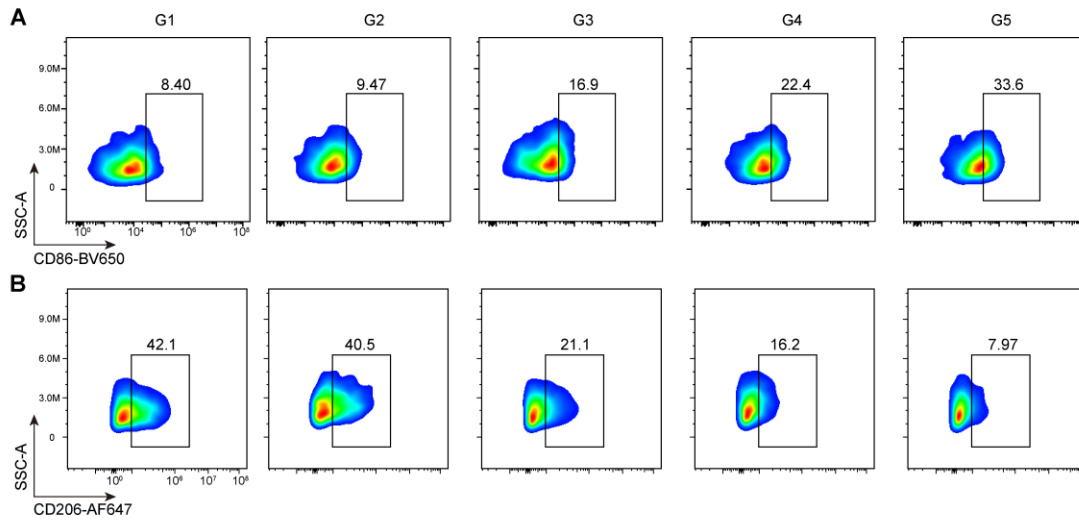


Fig. S19. Flow cytometry of tumor-infiltrating macrophage. (A) CD86⁺ CD206⁻ M1 phenotype macrophages within CD11b⁺ F4/80⁺ population. (B) CD86⁻ CD206⁺ M2 phenotype macrophages within CD11b⁺ F4/80⁺ population, $n = 4$. Related to Fig. 4.

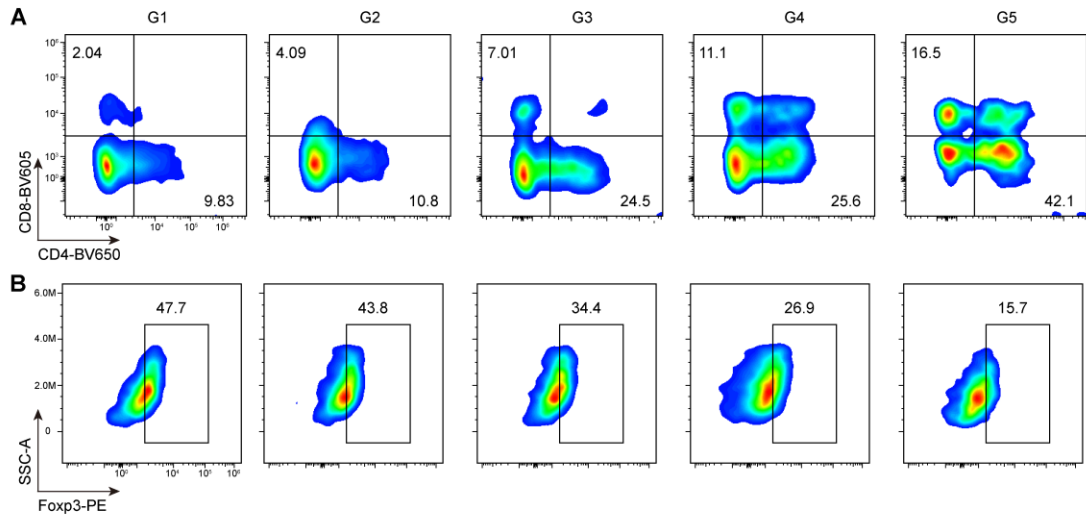


Fig. S20. Flow cytometry of tumor-infiltrating T cell. (A) CD8⁺ cytotoxic T cells within CD45⁺ CD3⁺ lymphocytes. (B) CD4⁺ Fcpx3⁺ regulatory T cells within CD45⁺ CD3⁺ lymphocytes, $n = 4$. Related to Fig. 4.

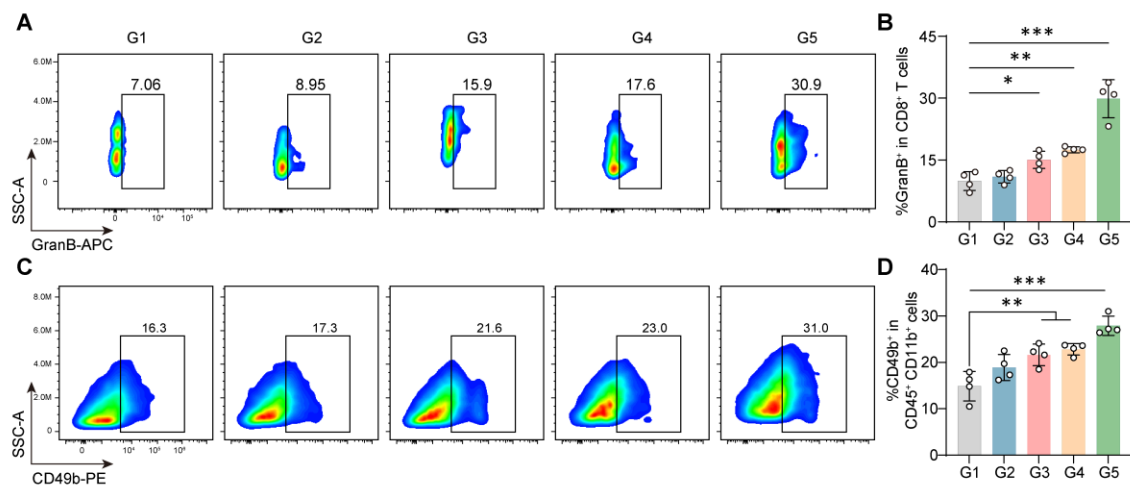


Fig. S21. Flow cytometry of Cytotoxic CD8⁺ T cells and NK cell. (A, B) Flow cytometry plots and quantification of Granzyme B⁺ cells in CD3⁺ CD8⁺ T cells. (C, D) Flow cytometry plots and quantification of CD49b⁺ NK cells in CD45⁺ CD11b⁺ population. Related to Fig. 4.

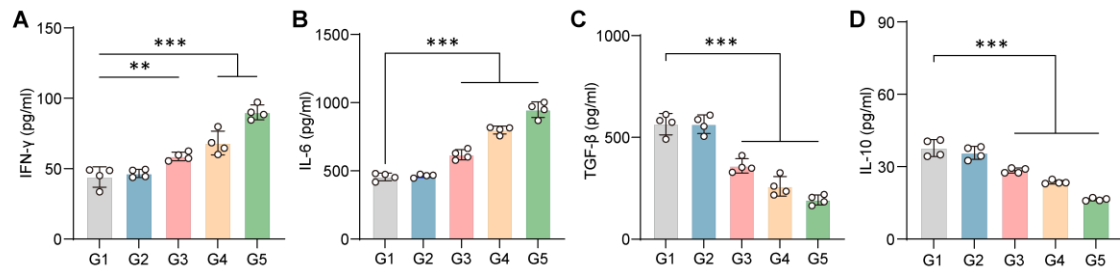


Fig. S22. Cytokine level in tumors. (A) IFN- γ levels in CT26 tumor. (B) IL-6 levels in CT26 tumor. (C) TGF- β levels in CT26 tumor. (D) IL-10 levels in CT26 tumor. $n=4$, ** $P < 0.01$, *** $P < 0.001$. Related to Fig. 4.

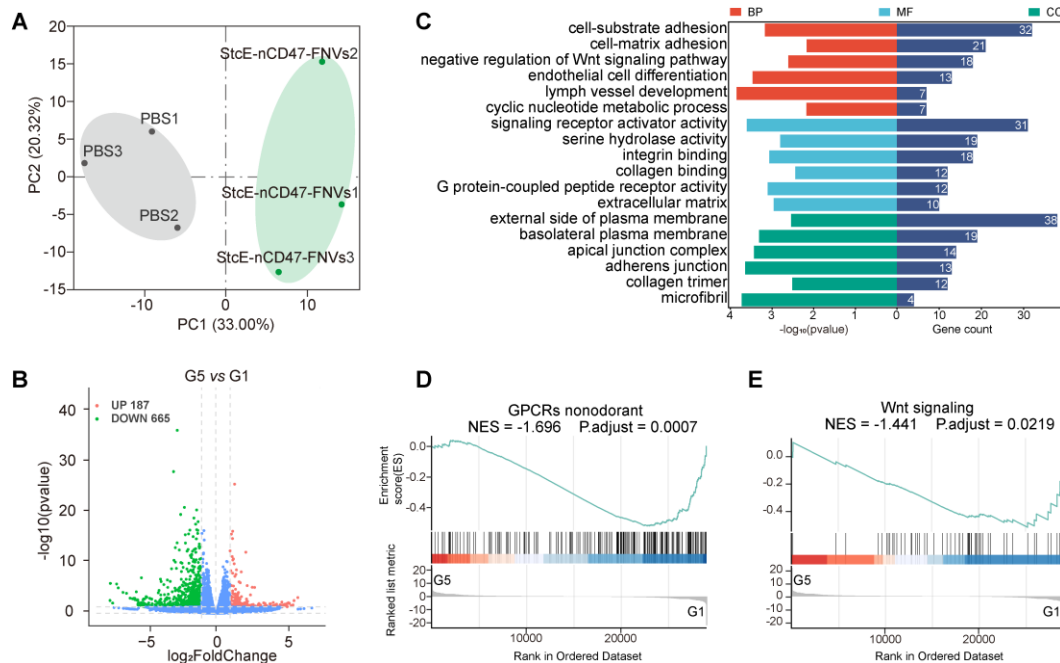


Fig. S23. RNA-sequencing analysis of tumor tissues from CT26 tumor-bearing mice after treatment. (A) Principal Component Analysis (PCA) plot of StcE-nCD47-FNVs group and PBS group. (B) Volcano plot of differentially expressed genes (DEGs) comparing CT26-StcE-nCD47-FNVs group with the Blank group. Upregulated and downregulated genes are indicated in red and green, respectively. (C) Gene Ontology (GO) analysis of DEGs between CT26-StcE-nCD47-FNVs group and Blank group. (D, E) Gene Set Enrichment Analysis (GSEA) of the "GPCRs nonodorant" (D) and "Wnt signaling" (E) pathways in G5 group. Related to Fig. 4.

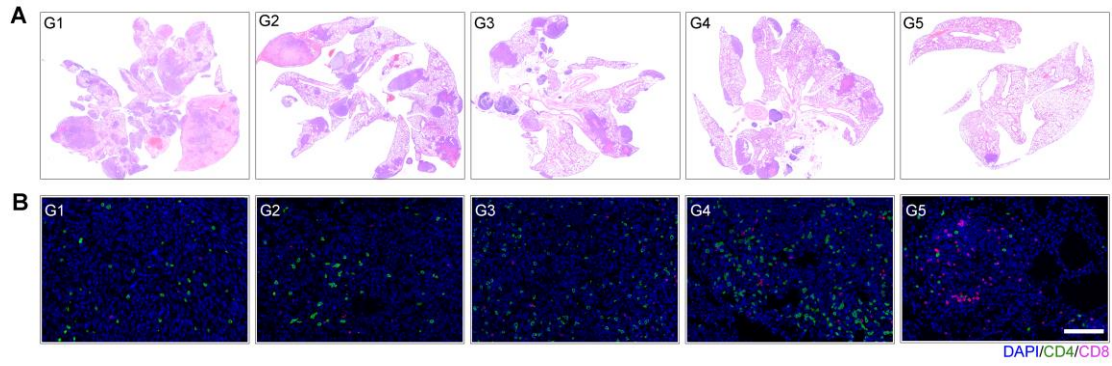


Fig. S24. Histological analysis of lung metastases after different treatments. (A) H&E-stained lung sections of different group. (B) Representative immunofluorescence images of infiltration of CD8⁺ T cells (red) and CD4⁺ T cells (green) in tumors. Scale bar, 100 μm. Related to Fig. 5.